Dynamics of driven two-level systems with permanent dipole moments: an optical realization

Dynamics of driven two-level systems with permanent dipole moments: an optical realization

Stefano Longhi

Dipartimento di Fisica and Istituto di Fotonica e Nanotecnologie del CNR, Politecnico di Milano, Piazza L da Vinci 32, I-20133 Milano, Italy

E-mail: longhi@fisi.polimi.it

Abstract
It is theoretically shown that the tunnelling dynamics of light between two sinusoidally curved coupled optical waveguides of different sizes exactly mimics the population dynamics of a two-level system with nonzero diagonal dipole matrix elements subjected to an applied sinusoidal electric field, thus realizing an optical analogue of a two-level dipolar molecule in an external ac field. Some characteristic dynamical features, including multi-photon transitions, sinusoidal population oscillations built up in a series of stair steps or square-wave population oscillations, are reproduced in the optical waveguide system. Design parameters for their observation are given with reference to lithium-niobate optical waveguides.

1. Introduction

In the understanding of the coherent interaction between radiation and matter, the two-level problem [1], in which two individual quantum states have interactions only with each other and with external fields, is perhaps the most basic and widely studied model. In the simplest and most studied case of atomic levels with a well-defined parity interacting with the electric field of an electromagnetic wave, the diagonal dipole matrix elements μ_{11} and μ_{22} vanish and, for a monochromatic wave and in the weak field regime, appreciable population transfer with typical sinusoidal periodicity (the familiar Rabi oscillations) is observed for electric-dipole allowed transitions solely when the frequency ω of the applied field is in resonance with the atomic transition frequency ω_0 (one-photon transition). A more complex population dynamics may occur for frequency modulated fields, including off-resonance complete population transfer [2], population trapping and square-wave oscillations [3, 4], or more complicated dynamical features associated with periodic level crossings [4–6]. The response of a two-level system with permanent dipole moments to an applied field, such as a dipolar molecule, shows additional and very appealing features, the most notable one being two-photon (or multi-photon) transitions which are forbidden for the two-level atom with $\mu_{11} = \mu_{22} = 0$ [7–11].

Many effects arising from permanent dipole moments on the two-level dynamics (polar two-level model) have been studied in the literature, especially in connection with dipolar molecules; among others, we just mention enhanced two-photon transitions [9, 12], nonlinear absorption and dispersion [13], harmonic generation [14–16], Raman scattering and wave mixing [17], optical bistability [18–20] and two-photon phase conjugation [21].

Owing to the strong similarities between light propagation in waveguide structures and electron dynamics in quantum systems [22, 23], photonic waveguides have been proven on many occasions to provide an ideal laboratory system to study coherent dynamical effects typical of quantum systems in the presence of external fields, such as optical Bloch oscillations [24], quantum tunnelling enhancement and suppression by external driving fields [25, 26], Landau–Zener dynamics [27, 28], wavepacket dichotomy and atomic stabilization [29] and coherent population transfer by stimulated Raman adiabatic passage [30]. By the use of a Kramers–Henneberger transformation it has been shown that the effect of an external ac driving field can be simulated in the optical waveguide system by introducing a periodic axis bending of the waveguide [26, 31]; in particular, two identical coupled waveguides with a periodic or aperiodic axis bending provide the optical analogue of a two-level atomic system with zero diagonal dipole matrix elements subjected to an applied frequency-modulated or frequency-swept field [26, 28]. The use of optical waveguides to study coherent quantum dynamics may offer a few advantages, such as the absence of dephasing effects that may destroy coherence [24], the possibility of observing the evolution dynamics as a stationary spatial field distribution along the propagation direction rather than as a fast temporal effect [24][1] and the possibility of investigating dynamical regimes not yet experimentally accessible in the atomic or molecular physics context [29].

In this paper, we propose an optical realization of a polar two-level molecular dynamics based on two single-mode coupled waveguides with different sizes and with a sinusoidally curved axis. Coupled-mode equations describing light propagation along the two waveguides are shown to be equivalent to those of a two-level system with permanent dipole moments, the periodic curvature of waveguide axis playing the role of the external coupling field. Some characteristic dynamical regimes of the polar two-level system, including light tunnelling due to multi-photon resonances and light dynamics that mimics periodic stair steps or square-wave population oscillations, are found in the optical waveguide system. The predictions based on the polar two-level model are confirmed by a direct numerical analysis of the original paraxial wave equation. The paper is organized as follows. In section 2 the basic model and the equivalence with the two-level dipolar molecule problem are presented. Section 3 presents the main results of light dynamics characteristic of the dipolar two-level model and provides design parameters for their observation in lithium-niobate waveguides. Finally, in section 4 the main conclusions are outlined.

2. Description of the optical system and the dipolar two-level model

2.1. The optical waveguide system

The optical system under investigation consists of two single-mode channel optical waveguides, with different designs and placed at a distance a, whose axis is not straight but it is periodically curved along the propagation z direction with a bending profile $x_0(z)$ (see figure 1). For strong guidance of light in the vertical y direction and weak guidance in the x direction, light propagation can be described by a scalar model for the electric field envelope

---

[1] The spatial evolution of light along straight or bent optical waveguides can be experimentally measured by the use of near-field scanning optical microscopy techniques, as demonstrated in several works (see, for instance, [32]).
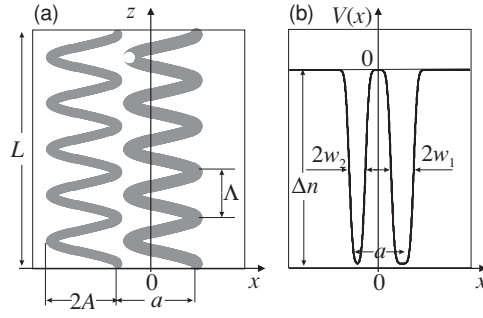
Figure 1. (a) Schematic of an asymmetric optical directional coupler made of two waveguides of different sizes with a sinusoidally curved axis. (b) Typical behaviour of the potential $V(x) = n_s - n(x)$ corresponding to the asymmetric directional coupler.

$\psi(x, z)$ using a parabolic paraxial wave equation for an effective nonuniform structure with a one-dimensional confinement only in the x direction (see, e.g., [33]). Precisely, the paraxial light propagation at wavelength $\lambda = 2\pi/k$ in the two optical waveguides can be described by an effective Schrödinger-like wave equation (see, e.g., [22, 26]):

$$\mathrm{i}\hbar \frac{\partial \psi}{\partial z} = -\frac{\hbar^2}{2n_s} \frac{\partial^2 \psi}{\partial x^2} + V(x - x_0(z))\psi, \tag{1}$$

where $\hbar \equiv \lambda/(2\pi) = 1/k$ is the reduced wavelength of light, $V(x) \equiv \left[n_s^2 - n^2(x)\right]/(2n_s) \simeq n_s - n(x)$, n_s is the substrate refractive index and $n(x)$ is the effective index profile of the coupler in the transverse x direction. Note that, identifying $\hbar$ with the Planck constant and z with time, equation (1) is equivalent to the Schrödinger equation for a particle of mass n_s in a periodically shaken potential $V(x)$, which describes the dynamics of a charged particle in the static potential $V(x)$ subjected to an external ac electric field in a Kramers–Henneberger reference frame (see, e.g. [31]). By means of a Kramers–Henneberger transformation

$$x' = x - x_0(z), \qquad z' = z, \tag{2}$$

$$\phi(x', z') = \psi(x', z') \exp\left[-\mathrm{i}\frac{n_s}{\hbar}\dot{x}_0 x' - \mathrm{i}\frac{n_s}{2\hbar} \int_0^{z'} \mathrm{d}\xi \, \dot{x}_0^2(\xi)\right] \tag{3}$$

(where the dot indicates the derivative with respect to z'), equation (1) takes in fact the form

$$\mathrm{i}\hbar \frac{\partial \phi}{\partial z'} = -\frac{\hbar^2}{2n_s} \frac{\partial^2 \phi}{\partial x'^2} + V(x')\phi - \mathcal{E}(z')x'\phi, \tag{4}$$

where

$$\mathcal{E}(z') \equiv -n_s \ddot{x}_0(z'), \tag{5}$$

provides the relationship between waveguide axis bending and amplitude of the external periodic driving field $\mathcal{E}(z')$ in the electric dipole approximation. In the following, we will assume for the sake of definiteness a sinusoidal bending profile (see figure 1(a)) with a spatial period Λ and an amplitude A, $x_0(z) = A\cos(2\pi z/\Lambda)$, corresponding to a sinusoidal applied electric field

$$\mathcal{E}(z') = \mathcal{E}_0 \cos(2\pi z/\Lambda), \tag{6}$$

with amplitude

$$\mathcal{E}_0 = 4\pi^2 n_s A/\Lambda^2. \tag{7}$$
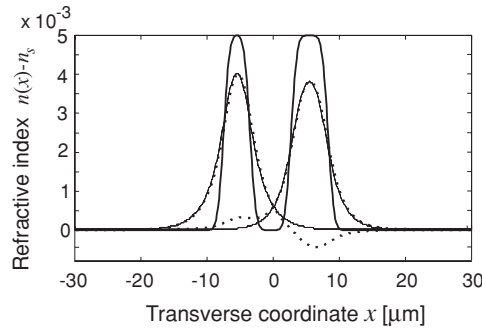
Figure 2. Refractive index profile (thick solid curve) and numerically computed profiles of the two supermodes (dotted curves) of a lithium-niobate waveguide coupler. The thin solid lines, partially overlapped with the dotted curves, are the profiles of the two individual waveguide modes. Parameter values are $n_s = 2.1381$, $\Delta n = 0.005$, $a = 11\,\mu$m, $w_1 = 2.8\,\mu$m, $w_2 = 2\,\mu$m, $D_x = 1\,\mu$m and $\lambda = 1.5\,\mu$m.

2.2. The Dipolar two-level model

In this section, we derive coupled mode equations describing light propagation in the two-waveguide coupler and show their equivalence with the standard two-level problem describing the dynamics of a two-level dipolar molecule subjected to an applied ac field [11]. To this aim, let us observe that, since the optical waveguides are assumed to have different widths and/or peak index changes (figure 1(b)), the potential $V(x)$ shows a typical asymmetric profile made of two different wells. In our analysis, we will assume that each waveguide of the coupler supports a single mode and that the full Hamiltonian of the straight coupler $\mathcal{H}_0 = -(\hbar^2/2n_s)\partial^2/\partial x^2 + V(x')$ admits solely two non-degenerate bound states (supermodes) $u_1(x)$ and $u_2(x)$ with propagation constants β_1 and β_2, i.e. $\mathcal{H}_0 u_{1,2}(x) = \hbar\beta_{1,2}u_{1,2}(x)$, with the normalization condition $\langle u_i | u_k \rangle = \delta_{ik}$ $(i, k = 1, 2)$. Since the two waveguides are of different designs, the two supermodes $u_1(x)$ and $u_2(x)$ are well approximated, at leading order, by the two individual waveguide modes, thus localizing light mostly in one of the two wells. This situation is very different from that of two identical waveguides, where the supermodes of the coupler are conversely quasi degenerate and well approximated by the symmetric and anti-symmetric linear combinations of the two individual waveguide modes [26][2].

In the numerical examples discussed in the following we will adopt for the sake of definiteness an effective refractive index profile for each waveguide of the form

$$n_w(x) = n_s + \Delta n \frac{\mathrm{erf}[(x + w_{1,2})/D_x] - \mathrm{erf}[(x - w_{1,2})/D_x]}{2\,\mathrm{erf}(w_{1,2}/D_x)}, \tag{8}$$

which applies to waveguides fabricated by diffusion processes [34]. In equation (8), $2w_1$ and $2w_2$ are the channel widths of the two waveguides, D_x is the lateral diffusion length and Δn is the peak refractive index change, which is assumed to be the same for the two waveguides. As an example, figure 2 shows the refractive index profile of a coupler and the numerically computed profiles of the two supermodes for parameter values which apply to lithium-niobate waveguides operating at $\lambda = 1.55\,\mu$m wavelength. Eigenvalue and eigenmode computation

---

[2] The asymmetry of the two waveguides plays a major role in the two-level dipolar molecule equivalence discussed in this work. In fact, for a symmetric waveguide coupler it was previously shown [26] that the light propagation is described by two-level equations analogous to those of a two-level atom ($\mu_{11} = \mu_{22} = 0$) subjected to a frequency-modulated field. The condition for destruction of light tunnelling reported in [26] is in fact analogous to the population trapping condition predicted, in the atomic physics context, in [3, 5].

have been performed by discretizing the operator $\mathcal{H}_0$ on a $60\,\mu$m wide domain with 512 grid points and by standard matrix eigenvalue computation of the discretized matrix operator. The eigenvalue analysis shows that the two-waveguide system does not support other bound modes and, as one can see from figure 2, each supermode confines light mostly in one of the two waveguides of the coupler.

To reduce the beam dynamics in the periodically curved waveguide coupler to a two-level problem, we neglect excitation of radiation (unbounded) modes and adopt a standard reduction procedure of the dynamics on the basis of $u_1(x')$ and $u_2(x')$ states. After setting

$$\phi(x', z') = a_1(z')u_1(x')\exp(-\mathrm{i}\beta_{av}z') + a_2(z')u_2(x')\exp(-\mathrm{i}\beta_{av}z'), \tag{9}$$

where $\beta_{av} \equiv (\beta_1 + \beta_2)/2$, using the orthonormal properties $\langle u_i|u_k\rangle = \delta_{i,k}$, substitution of equation (9) into equation (4) yields

$$\mathrm{i}\frac{\mathrm{d}}{\mathrm{d}z'}\begin{pmatrix} a_1 \\ a_2 \end{pmatrix} = \begin{pmatrix} \frac{\Delta\beta}{2} & 0 \\ 0 & -\frac{\Delta\beta}{2} \end{pmatrix}\begin{pmatrix} a_1 \\ a_2 \end{pmatrix} - \frac{\mathcal{E}(z')}{\hbar}\begin{pmatrix} \mu_{11} & \mu_{12} \\ \mu_{21} & \mu_{22} \end{pmatrix}\begin{pmatrix} a_1 \\ a_2 \end{pmatrix}, \tag{10}$$

where we have set $\mu_{ik} \equiv \langle u_i|x'|u_k\rangle$ $(i, k = 1, 2)$ and $\Delta\beta \equiv \beta_1 - \beta_2$. In the present form, equations (10) exactly describe the dynamics of a two-level system with permanent dipole moments, such as a two-level dipolar molecule, interacting with a time-dependent electric field $\mathcal{E}(z')$ in the electric dipole approximation, the energy separation between the two involved quantum states being $\hbar\Delta\beta$ (see, e.g., [11, 16, 20]). Note that $\mu_{12} = \mu_{21}^*$ can be assumed to be real valued and related to an integral overlap of adjacent waveguide modes, whereas the diagonal dipole matrix elements μ_{11} and μ_{22} do not vanish and, at leading order, are given by $\mu_{11} \sim -\mu_{22} \sim a/2$, where a is the separation between the two waveguides. For two waveguides not too close to each other, one then has $|\mu_{12}| \ll |\mu_{22} - \mu_{11}|$, i.e. the two level system is strongly dipolar. Note also that, as in the quantum physics context $|a_1|^2$ and $|a_2|^2$ describe the populations in the two quantum molecular levels, in our optical systems $|a_1|^2$ and $|a_2|^2$ are basically the fractional light power trapped into the two waveguides. Different though equivalent forms for the two-level equations (10) can be considered [8, 11, 16, 19, 20], which may be more suited to study the two-level dynamics under the rotating-wave approximation (for a fast field oscillation) or in the adiabatic limit (for a slow field oscillation). After the phase transformation

$$a_{1,2}(z') = \bar{a}_{1,2}(z')\exp\left[\mathrm{i}\frac{\mu_{11} + \mu_{22}}{2\hbar}\int_0^{z'}\mathcal{E}(\xi)\,\mathrm{d}\xi\right], \tag{11}$$

one obtains the second form for the polar two-level problem:

$$\mathrm{i}\frac{\mathrm{d}}{\mathrm{d}z'}\begin{pmatrix} \bar{a}_1 \\ \bar{a}_2 \end{pmatrix} = \begin{pmatrix} -\varphi(z') & 0 \\ 0 & \varphi(z') \end{pmatrix}\begin{pmatrix} \bar{a}_1 \\ \bar{a}_2 \end{pmatrix} - \frac{\mathcal{E}(z')}{\hbar}\begin{pmatrix} 0 & \mu_{12} \\ \mu_{21} & 0 \end{pmatrix}\begin{pmatrix} \bar{a}_1 \\ \bar{a}_2 \end{pmatrix}, \tag{12}$$

where we have set

$$\varphi(z') \equiv -\frac{\Delta\beta}{2} + \frac{\mu_{11} - \mu_{22}}{2\hbar}\mathcal{E}(z'). \tag{13}$$

Equations (12) and (13) clearly show that, if the two-level system has permanent dipoles and if $\mu_{11} \neq \mu_{22}$, the applied electric field not only couples the two states through the off-diagonal dipole matrix element μ_{12}, but also modulates the energy separation of the two levels around the value $\hbar\Delta\beta$. In particular, for strong fields periodic level crossing, corresponding to $\varphi(z') = 0$, can be attained. A third form for the polar two-level problem can be finally obtained after the further phase transformation

$$\bar{a}_{1,2}(z') = c_{1,2}(z')\exp\left[\pm\mathrm{i}\frac{\theta(z')}{2}\right], \tag{14}$$

where

$$\theta(z') \equiv 2 \int_0^{z'} \varphi(\xi) \, \mathrm{d}\xi = -\Delta\beta z' + \frac{\mu_{11} - \mu_{22}}{\hbar} \int_0^{z'} \mathcal{E}(\xi) \, \mathrm{d}\xi. \tag{15}$$

One obtains the third form for the two-level equations

$$\mathrm{i}\frac{\mathrm{d}}{\mathrm{d}z'} \begin{pmatrix} c_1 \\ c_2 \end{pmatrix} = -\frac{\mathcal{E}(z')}{\hbar} \begin{pmatrix} 0 & \mu_{12}\exp[-\mathrm{i}\theta(z')] \\ \mu_{21}\exp[\mathrm{i}\theta(z')] & 0 \end{pmatrix} \begin{pmatrix} c_1 \\ c_2 \end{pmatrix}. \tag{16}$$

The last form of the polar two-level problem is suited for an application of the rotating-wave approximation in the high-frequency limit [7, 11, 16, 20].

3. Light tunnelling dynamics

In this section we present a few optical tunnelling effects in the periodically curved asymmetric waveguide coupler that provide the optical analogue of corresponding population dynamic effects of the dipolar two-level model (equations (10), (12) or (16)) previously studied mainly in the context of dipolar molecules. The general solution to the two-level equations for a sinusoidal driving field $\mathcal{E}(z') = \mathcal{E}_0 \cos(2\pi z'/\Lambda)$ can be obtained for general parameter values only by direct numerical simulations, using the Floquet theory of periodic systems. There are nevertheless two limiting cases that deserve particular attention: the high-frequency modulation and low-field limit, in which population transfer effectively occurs under certain resonance conditions (multi-photon transitions), and the low-frequency modulation and strong-field limit, in which the population dynamics is mainly governed by periodic level crossings. In the former case, one can employ a rotating-wave (or averaging) approximation to obtain approximate analytical results; one of the major results of the analysis is that, as opposed to the non-polar (atomic) two-level model, a two-photon (or multi-photon) transition is allowed in the dipolar two-level model (dipolar molecule) [7, 11]. The population dynamics in the low-frequency modulation limit is mainly governed by periodic level crossing and is expected therefore to show similar features (such as square-wave population oscillations) to those observed in the non-polar (atomic) two-level model subjected to frequency-modulated laser fields [3, 6] or related two-level models (see, e.g. [4, 35]).

3.1. Multi-photon transitions

For periodically curved waveguides, from equations (15) and (16) one can see that the coupling term $I(z') \equiv -[\mu_{12}\mathcal{E}(z')/\hbar]\exp[-\mathrm{i}\theta(z')]$ between states c_1 (light trapped in the right waveguide) and c_2 (light trapped in the left waveguide) contains terms oscillating at frequencies $-\Delta\beta + l\Omega$, where $\Omega = 2\pi/\Lambda$ is the spatial modulation frequency and l is an integer number. If the frequency Ω is sufficiently larger than the coupling term $\mu_{12}\mathcal{E}_0/\hbar$, the rapidly oscillating terms do not contribute effectively to the coupling between the two states, unless a resonance condition $n\Omega \sim \Delta\beta$ is satisfied for some integer n. In this case, the leading-order evolution equations describing the mode coupling can be obtained by averaging the coupling term $I(z')$ over the spatial period Λ (rotating-wave approximation), i.e. one can write

$$\mathrm{i}\frac{\mathrm{d}}{\mathrm{d}z'} \begin{pmatrix} c_1 \\ c_2 \end{pmatrix} = \begin{pmatrix} 0 & \langle I(z') \rangle \\ \langle I(z')^* \rangle & 0 \end{pmatrix} \begin{pmatrix} c_1 \\ c_2 \end{pmatrix}, \tag{17}$$

where the bracket denotes a spatial average. Taking into account equation (15), by an integration by parts one can readily show that one can write

$$\langle I(z') \rangle = -\frac{\mu_{12}}{\hbar} \langle \mathcal{E}(z')\exp[-\mathrm{i}\theta(z')] \rangle = \Delta\beta \frac{\mu_{12}}{\mu_{22} - \mu_{11}} \langle \exp[-\mathrm{i}\theta(z')] \rangle, \tag{18}$$

that is

$$\langle I(z')\rangle = \Delta\beta \frac{\mu_{12}}{\mu_{22} - \mu_{11}} \left\langle \exp\left[i\Delta\beta z' + i\frac{\mu_{22} - \mu_{11}}{\hbar} \int_0^{z'} \mathcal{E}(\xi)\, d\xi \right] \right\rangle. \qquad (19)$$

In particular, for a sinusoidal field, $\mathcal{E}(z') = \mathcal{E}_0 \cos(\Omega z')$, assuming the n-photon resonance condition ($n\Omega \sim \Delta\beta$), one has (see also [7, 11, 16, 19])

$$\langle I(z')\rangle = \Delta\beta \frac{\mu_{12}}{\mu_{22} - \mu_{11}} J_n(\kappa) \exp[i(\Delta\beta - n\Omega)z'], \qquad (20)$$

where J_n is the Bessel function of order n and where we have set

$$\kappa \equiv \frac{(\mu_{11} - \mu_{22})\mathcal{E}_0}{\hbar\Omega} = \frac{4\pi^2 n_s A(\mu_{11} - \mu_{22})}{\lambda\Lambda}. \qquad (21)$$

In this case the solution to equations (17) shows a typical sinusoidal Rabi flopping, corresponding to periodic tunnelling of light between the two coupled waveguides, with complete light tunnelling in the perfect resonance case, provided that $J_n(\kappa) \neq 0$. In fact, the solution to equations (17) corresponding to the initial excitation of the right waveguide ($c_1(0) = 1, c_2(0) = 0$) is given by [1]

$$c_1(z') = \left[\cos(\Omega_R z') - i\frac{\delta}{\Omega_R} \sin(\Omega_R z') \right] \exp(i\delta z'), \qquad (22)$$

$$c_2(z') = -i\frac{\sigma}{\Omega_R} \sin(\Omega_R z') \exp(-i\delta z'), \qquad (23)$$

where we have set $\delta \equiv (\Delta\beta - n\Omega)/2$, $\sigma \equiv \mu_{12}\Delta\beta J_n(\kappa)/(\mu_{22} - \mu_{11})$ and $\Omega_R \equiv (\sigma^2 + \delta^2)^{1/2}$. The fractional power of light tunnelled in the left waveguide thus changes periodically during propagation, at a frequency $2\Omega_R$, according to

$$|c_2(z')|^2 = \frac{\sigma^2}{\sigma^2 + \delta^2} \sin^2(\Omega_R z'), \qquad (24)$$

and complete tunnelling occurs in the perfect resonance case $\delta = 0$. Note that, as the modulation amplitude A (or field strength $\mathcal{E}_0$, see equation (7)) is increased from zero to reach the condition $J_n(\kappa) = 0$, light tunnelling is inhibited within the rotating-wave approximation, a condition which is similar to coherent destruction of tunnelling in the symmetric optical directional coupler [26].

We checked the validity of the polar two-level model to describe the tunnelling light dynamics in the sinusoidally curved asymmetric optical directional coupler by a direct numerical integration of the paraxial wave equation describing beam propagation. For the sake of simplicity and readability of the results, we integrated the paraxial wave equation in the Kramers–Henneberger reference frame (equations (2)–(4)), where the two waveguides appear to be straight. A standard split-step beam propagation technique has been used to integrate equation (4), with absorbing boundary conditions to simulate radiation losses and with typical 1024 discretization points in the transverse x' direction (for more details see [31]). The geometry and parameters of the asymmetric waveguide coupler used in the numerical simulations are shown in figure 2, which apply to a typical lithium-niobate waveguide coupler operating at the 1.5 μm wavelength of optical communications. For such a structure, numerical computation of supermodes and corresponding dipole matrix elements yields the numerical values $\mu_{11} \simeq 5.42\,\mu$m, $\mu_{22} \simeq -5.41\,\mu$m and $\mu_{12} \simeq -1.01\,\mu$m. The propagation constant difference turns out to be $|\Delta\beta| = 3.073\,\text{mm}^{-1}$, so that n-photon resonance is attained for a sinusoidal axis bending modulation of period $\Lambda_n \simeq 2.045 \times n$ (mm). As an example,
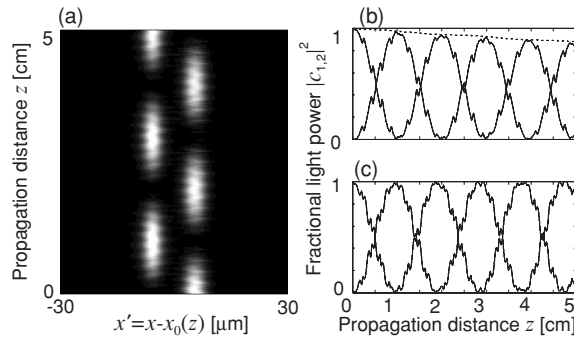
Figure 3. (a) Numerically computed beam evolution in a $L = 5$ cm long asymmetric waveguide coupler corresponding to one-photon resonance. Parameter values of sinusoidal bending are $\Lambda = 2045\,\mu$m and $A = 6\,\mu$m (corresponding to $\kappa \sim 1.79$). The other design parameters of the coupler are the same as in figure 2. (b) Numerically computed behaviour of the fractional beam power in the two waveguides (solid lines) versus propagation distance. The dashed line in the figure represents the total beam power, normalized to its input value, contained in the $60\,\mu$m wide transverse integration domain. (c) Behaviour of the fractional beam power in the two waveguides as obtained by a numerical analysis of the dipolar two-level equation (10).
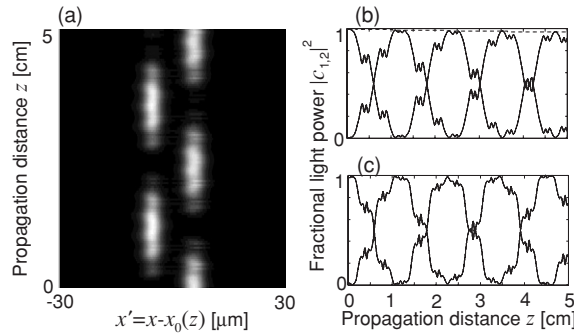
Figure 4. Same as figure 3, but for parameter values corresponding to two-photon resonance ($\Lambda = 4090\,\mu$m and $A = 20\,\mu$m, corresponding to $\kappa \sim 2.98$).

figures 3(a) and 4(a) show snapshots of the numerically computed beam intensity evolution $|\phi(x', z')|^2$ along a $L = 5$ cm long waveguide coupler for parameter values corresponding to one-photon (figure 3(a)) and two-photon (figure 4(a)) resonances when the right waveguide is excited at the entrance facet in its fundamental mode. Figures 3(b) and 4(b) show the corresponding fractional beam power localized in each of the two waveguides along the propagation distance (calculated as $|c_k(z')|^2 = |\langle \phi | u_k \rangle|^2$), together with the total beam power, normalized to its input value, contained in the transverse integration domain (dashed curves). Note that, for the chosen parameter values, radiation losses are kept at a low level and, for exact resonances ($\delta = 0$) as in the figures, complete light tunnelling oscillations are observed with a periodicity which is very close to the analytical value predicted within the dipolar two-level model. The obtained numerical results, based on a direct numerical integration of the paraxial wave equation (4), turn out to be in good agreement with those predicted by the dipolar two-level model. This is shown in figures 3(c) and 4(c), where the evolution of fractional beam power $|c_k(z')|^2$ in the two waveguides is reported as numerically computed
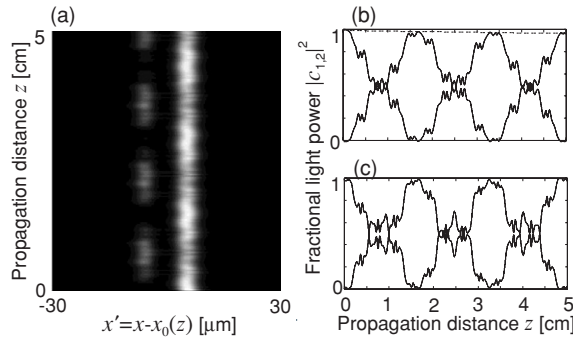
Figure 5. Same as figure 4, but for parameter values corresponding to a detuned two-photon resonance ($\Lambda = 3800\,\mu$m and $A = 20\,\mu$m, corresponding to $\kappa \sim 3.2$).
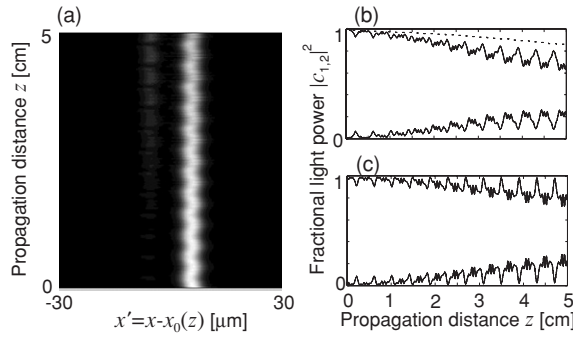
Figure 6. Same as figure 4 (two-photon resonance) but for parameter values corresponding to a zero of Bessel function J_2 ($\Lambda = 4090\,\mu$m and $A = 34.5\,\mu$m, corresponding to $\kappa \sim 5.14$).

by integration of equations (10) using a fourth-order Runge–Kutta technique. According to the theoretical analysis (see equation (24)), we observed periodic light tunnelling between the two waveguides even under a detuned condition ($\delta \neq 0$); however in this case the tunnelling is incomplete, as shown in figure 5. The rotating-wave approximation predicts suppression of tunnelling when the effective coupling parameter κ (equation (21)) is a root of the Bessel function J_n. As an example, figure 6 shows the suppression of resonant light tunnelling at the two-photon resonance when the modulation amplitude A of axis bending is increased, from the value of figure 4, to reach the first root of the Bessel function J_2 ($\kappa \sim 5.14$).

3.2. Square-wave tunnelling

As the spatial modulation period Λ increases, the high-frequency and rotating-wave approximations introduced in the previous section fail to correctly describe the tunnelling dynamics of light between the two waveguides, and a direct numerical analysis of equations (10) is in order. The failure of the rotating-wave approximation is clearly visible when considering higher-order resonance conditions: as the spatial modulation frequency $\Omega = 2\pi/\Lambda$ decreases, from e.g. the one-photon to the three-photon resonance (see figures 3, 4 and 7), the tunnelling oscillations of light between the two waveguides change from
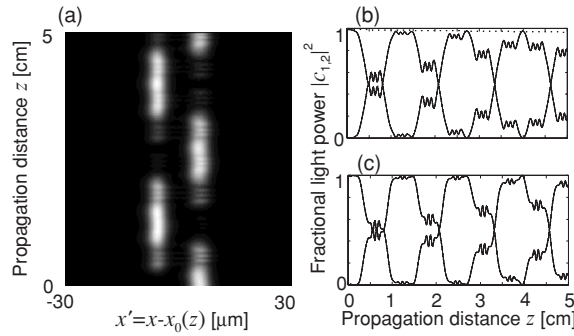
Figure 7. Same as figure 3, but for parameter values corresponding to a three-photon resonance ($\Lambda = 6135\,\mu$m and $A = 40\,\mu$m, corresponding to $\kappa \sim 3.97$).

a periodic and nearly sinusoidal profile, as predicted by the rotating-wave approximation (figure 3), to a sinusoidal oscillation built up in a series of stair steps (figures 4 and 7) which may become aperiodic (figure 7). In the low-frequency modulation limit from equations (12) one can see that, for a field strength $\mathcal{E}_0$ larger than $\hbar|\Delta\beta|/|\mu_{11}-\mu_{22}|$, one obtains a picture of periodic level crossing (see, e.g. [4, 6, 35]). In each modulation period, there are two positions z' at which the energy separation $2\hbar\varphi(z')$ of the two levels vanishes: between two successive crossings one has adiabatic following, and for sufficiently high values of $|\varphi(z')|$ (namely, for $|\varphi(z')| \gg |\mu_{12}\mathcal{E}_0/\hbar|$) light tunnelling between the waveguides is basically inhibited. Nonadiabatic transitions, corresponding to non-negligible Landau–Zener tunnelling of light between the waveguides, may occur at each linear level crossing[3]. Though a semi-quantitative analysis of tunnelling dynamics might be obtained by the use of nonadiabatic techniques (see, e.g. , [6]) and different dynamical effects may be observed, here we just limit ourselves to show, by a direct numerical analysis of equations (12), the existence of periodic square-wave tunnelling, corresponding to square-wave population oscillations in the quantum analogy. To this aim, let us note that in the general case the light tunnelling dynamics turns out to be aperiodic: in fact, indicating by $\pm \mathrm{i}f$ (with f real-valued) the Floquet exponents of the periodic system (12), the condition for periodicity is attained whenever the product $f\Lambda$ is a fractional multiple of 2π.[4] Such a condition may be realized for special design parameters of the waveguide coupler, as will be shown below. An example of periodic tunnelling dynamics, corresponding to square-wave oscillations, is shown in figure 8 for a waveguide coupler of length $L = 8$ cm, modulation period $\Lambda = 17$ mm and with the same refractive index profile as in figure 2. For the chosen modulation period Λ and for the modulation amplitude A leading to a period tunnelling dynamics, the two crossing points in each modulation cycle are very close to each other (see figure 8(d)), so that tunnelling may effectively occur in the short distance separating the two crossing points, where the energy level separation $2\hbar\varphi(z')$ is small. This is clearly visible with the help of figures 8(c) and (d), in which the evolution of the

---

[3] If the field strength $\mathcal{E}_0$ is close to $\hbar\Delta\beta/|\mu_{11} - \mu_{22}|$, the two crossing points in each period are close to each other and nonadiabatic effects result from a parabolic (rather than linear) level crossing. This is the case, for instance, considered in figure 8 depicting square-wave tunnelling oscillations.

[4] According to the Floquet theory, the propagator $\Phi(z')$ that maps the state of system (12) at initial position $z' = 0$ to its state at position z', $\bar{\mathbf{a}}(z') = \Phi(z')\bar{\mathbf{a}}(0)$ (where $\bar{\mathbf{a}} = (\bar{a}_1, \bar{a}_2)^T$), has the form $\Phi(z') = \exp(\mathcal{R}z')\mathcal{P}(z')$, where $\mathcal{P}(0) = \mathcal{I}$ is the identity matrix, $\mathcal{P}(z' + \Lambda) = \mathcal{P}(z')$ and $\mathcal{R}$ is a z'-independent 2×2 matrix whose eigenvalues $\pm \mathrm{i}f$ are the Floquet exponents. If there exist two irreducible integers m and n such that $nf\Lambda = 2\pi m$, then one has $\Phi(n\Lambda) = \exp(\mathcal{R}n\Lambda) = \mathcal{I}$, so that $\bar{\mathbf{a}}(n\Lambda) = \bar{\mathbf{a}}(0)$, i.e. the solution is periodic with period $n\Lambda$.
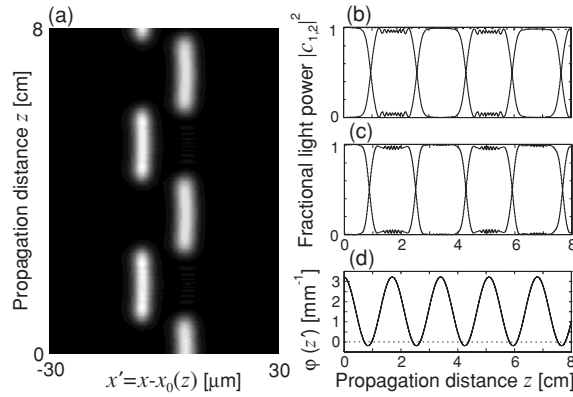
Figure 8. Same as figure 3, but for parameter values leading to square-wave tunnelling oscillations ($\Lambda = 17\,\text{mm}$ and $A = 260\,\mu\text{m}$; the waveguide length is now $L = 8\,\text{cm}$). Part (d) shows the behaviour of the local two-level separation $\varphi(z')$ (see equation (13)), with periodic level crossing at the intersections with the dashed horizontal line.
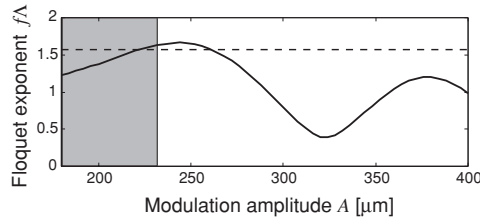
Figure 9. Numerically computed Floquet exponent f, normalized to the inverse of the modulation period Λ, versus bending modulation amplitude A for a waveguide coupler with parameter values as in figure 8. The horizontal dashed line corresponds to $f = \pi/(2\Lambda)$ (Λ periodic solution). The shaded area corresponds to the values of A for which level crossing is prevented.

fractional beam power in each waveguide is plotted and compared to the local level separation $\varphi(z')$. The amplitude A of waveguide bending leading to a periodic tunnelling dynamics can be determined by a numerical computation of the Floquet exponent f versus the amplitude A; the behaviour of the curve $f = f(A)$ is shown in figure 9. The shaded region in the figure corresponds to low amplitude values for which level crossing does not occur, whereas the horizontal dashed line corresponds to $\Lambda = \pi/2$. Note that, for such a particular value of the Floquet exponent (attained at $A \simeq 260\,\mu\text{m}$, the value of A used in the plots of figure 8), the functions $c_k(z')$ turn out to be periodic (both phase and amplitude) with period 4Λ. As shown in figure 8(c), the periodicity of $|c_k(z')|^2$ is nevertheless given by 2Λ.

4. Conclusions

To conclude, in this work we have theoretically shown that light propagation in an asymmetric optical directional coupler with a sinusoidally curved axis provides an interesting optical realization of a polar two-level quantum system, such as a two-level dipolar molecule. Design parameters for the observation of typical coherent dynamical effects of dipolar two-level systems, including multi-photon resonances and square-wave population oscillations, have

been provided for a lithium-niobate optical directional coupler. As waveguide-based optical systems have been shown in recent years to provide an ideal laboratory system to study coherent dynamical effects in solid-state [24, 27] or atomic [29, 30] quantum systems, the present analysis indicates that optical waveguides can be designed and used also to realize in an optical system coherent quantum effects typical of dipolar molecules.

References

[1] Allen L and Eberly J H 1987 *Optical Resonance and Two-level Atoms* (New York: Dover)
[2] Lam P K and Savage C M 1994 *Phys. Rev.* A **50** 3500
[3] Agarwal G S and Harshawardhan W 1994 *Phys. Rev.* A **50** R4465
[4] Noel M W, Griffith W M and Gallagher T F 1998 *Phys. Rev.* A **58** 2265
[5] Raghavan S, Kenkre V M, Dunlap D H, Bishop A R and Salkola M I 1996 *Phys. Rev.* A **54** R1781
[6] Garraway B M and Vitanov N V 1997 *Phys. Rev.* A **55** 4418
[7] Kmetic M A and Meath W J 1985 *Phys. Lett.* A **108** 340
[8] Kmetic M A, Thuraisingham R A and Meath W J 1986 *Phys. Rev.* A **33** 1688
[9] Band Y B, Bavli R and Heller D F 1989 *Chem. Phys. Lett.* **156** 405
[10] Kmetic M A and Meath W J 1990 *Phys. Rev.* A **41** 1556
[11] Brown A, Meath W J and Tran P 2000 *Phys. Rev.* A **63** 013403
[12] Scharf B E and Band Y B 1988 *Chem. Phys. Lett.* **144** 165
[13] Bavli R and Band Y B 1991 *Phys. Rev.* A **43** 5039
[14] Bavli R and Band Y B 1991 *Phys. Rev.* A **43** 507
[15] Andrews D L and Meath W J 1993 *J. Phys. B: At. Mol. Opt. Phys.* **26** 4633
[16] Calderon O G, Gutierrez-Castrejon R and Guerra J M 1999 *IEEE J. Quantum Electron.* **35** 47
[17] Bavli R, Heller D F and Band Y B 1990 *Phys. Rev.* A **41** 3960
[18] Kobayashi T, Kothari N C and Uchiki H 1984 *Phys. Rev.* A **29** 2727
[19] Anton M A and Gonzalo I 1995 *IEEE J. Quantum Electron.* **31** 1088
[20] Calderon O G, Melle S and Gonzalo I 2002 *Phys. Rev.* A **65** 023811
[21] Hoerner C, Lavoine J P and Villaeys A A 1993 *Phys. Rev.* A **48** 1564
[22] Kawano K and Kitoh T 2001 *Introduction to Optical Waveguide Analysis: Solving Maxwell's Equations and The Schrödinger Equation* (New York: Wiley-Interscience)
[23] März R 1995 *Integrated Optics: Design and Modeling* (Boston, MA: Artech House Publishers)
[24] Morandotti R, Peschel U, Aitchison J S, Eisenberg H S and Silberberg Y 1999 *Phys. Rev. Lett.* **83** 4756
     Pertsch T, Dannberg P, Elflein W, Bräuer A and Lederer F 1999 *Phys. Rev. Lett.* **83** 4752
     Lenz G, Talanina I and de Sterke C M 1999 *Phys. Rev. Lett.* **83** 963
[25] Vorobeichik I, Narevicius E, Rosenblum G, Orenstein M and Moiseyev N 2003 *Phys. Rev. Lett.* **90** 176806
[26] Longhi S 2005 *Phys. Rev.* A **71** 065801
[27] Khomeriki R and Ruffo S 2005 *Phys. Rev. Lett.* **94** 113904
[28] Longhi S 2005 *J. Opt. B: Quantum Semiclass. Opt.* **7** L9
[29] Longhi S, Marangoni M, Janner D, Ramponi R, Laporta P, Cianci E and Foglietti V 2005 *Phys. Rev. Lett.* **94** 073002
[30] Longhi S 2006 *Phys Rev. E* **73** 026607
[31] Longhi S, Janner D, Marano M and Laporta P 2003 *Phys. Rev. E* **67** 036601
[32] Yuan G, Lear L, Stephens M D and Dandy D S 2005 *Appl. Phys. Lett.* **87** 191107
[33] Sukhorukov A A, Kivshar Y S, Eisenberg H S and Silberberg Y 2003 *IEEE J. Quantum Electron.* **39** 31
[34] Sharma A and Bindal P 1992 *Opt. Quantum Electron.* **24** 1359
[35] Gauthey F I, Garraway B M and Knight P L 1997 *Phys. Rev.* A **56** 3093